Journal of Thermal Analysis and Calorimetry, Vol. 67 (2002) 721–731

DSC MONITORING OF THE SPIN CROSSOVER IN Fe(II) COMPLEXES

B. Papánková[1], *M. Vrbová*[1], *R. Boča*[1], *P. Šimon*[2], *K. Falk*[3], *G. Miehe*[4] *and H. Fuess*[4]

[1]Department of Inorganic Chemistry, Slovak Technical University, SK–812 37 Bratislava, Slovakia
[2]Department of Physical Chemistry, Slovak Technical University, SK–812 37 Bratislava, Slovakia
[3]Institute of Physical Chemistry, Darmstadt University of Technology, D–64289 Darmstadt, Germany
[4]Institute of Material Science, Darmstadt University of Technology, D–64289 Darmstadt, Germany

(Received June 6, 2001)

Abstract

Heat flow to $[Fe(bzimpy)_2](ClO_4)_2 \cdot 0.25H_2O$ complex (*bzimpy*=2,6-bis(benzimidazol-2-yl)pyridine) (**I**) was measured between 300 and 460 K by differential scanning calorimetry. This exhibits a well-developed peak characteristic of the first-order phase transitions at temperature 403 K. The enthalpy and entropy of transition from low-spin to high-spin state has been determined to be ΔH=17 kJ mol^{-1} and ΔS=43.0 J mol^{-1} K^{-1}. Heat flow to $[Fe(bzimpy_{-1H})_2] \cdot H_2O$ complex ($bzimpy_{-1H}$= deprotonated bzimpy) (**II**) was measured between 300 and 580 K. The spin crossover in this system is accompanied with liberation of crystal water on the first heating. To monitor the structural changes during the spin crossover, powder diffraction data have been collected as a function of temperature.

Keywords: DSC, iron(II) complexes, spin-crossover, X-ray powder diffraction

Introduction

Spin transition complexes have a potential application as thermal or optical switching devices and eventually memory units [1–3]. An important requirement is that the spin transition occurs near or above room temperature and possesses a broad hysteresis providing the temperature memory of the material.

Some molecular systems containing metal ion with the $3d^n$ (n=4 to 7) electronic configuration can form complexes in at least two different spin states. Iron(II) is a typical example: in an octahedral field it can be either high spin (HS, S=2) or low spin (LS, S=0), depending on the strength of the ligand field. Ligands generating strong crystal field favor the LS state, whereas weak-field ligands stabilize the HS state. Ligands of an intermediate-field strength can give rise to compounds, which are LS (say $^1A_{1g}$) in the ground state and HS (e.g. $^5T_{2g}$) in the excited state. The enthalpy change

1418–2874/2002/ $ 5.00
Akadémiai Kiadó, Budapest

on the spin transition $\Delta H \approx (E_{HS}^{el} - \varepsilon_{HS}^{vib}) - (E_{LS}^{el} - \varepsilon_{LS}^{vib})$ is positive. The entropy change ΔS includes a spin contribution $\Delta S_{spin} = R\ln(g_{HS}/g_{LS})$, as well as a vibrational contribution ΔS_{vib} (which is substantial). As a result of positive ΔH and positive ΔS, the Gibbs energy change adopts a negative value above a transition temperature $T_c = \Delta H/\Delta S$ when the spin transition becomes a spontaneous process.

Iron(II) complexes with the ligand 2,6-bis(benzimidazol-2-yl)pyridine (bzimpy) show the spin crossover (S=0 to S=2 transition) above room temperature. $[Fe(bzimpy)_2](BPh_4)_2 \cdot 4H_2O$ complex transforms at T_c=330 but on overheating to 400 K it loses its crystal water and remains high-spin [4]. $[Fe(bzimpy)_2](ClO_4)_2 \cdot 0.25H_2O$ exhibits a very sharp spin transition at T_c=403 K accompanied with a hysteresis width of ΔT=12 K [5]. The deprotonated species $[Fe(bzimpy_{-1H})_2] \cdot H_2O$ loses its crystal water on the first heating along with the spin transition centered at T_c=470 K [6].

The fact that the magnetic susceptibility is a thermodynamic quantity measured at the thermal equilibrium is often overlooked and relatively few sources of information in this respect are at disposal [7–12]. According to [8] the magnetic information is complete only when the magnetic susceptibility data are completed by the heat capacity measurements.

Following the pioneering work [13] we focused our attention in the present paper on thermodynamic aspects of the spin crossover. The situation is a bit more complex due to the fact that the Gibbs energy contains not only the enthalpic and entropic contributions but also a cooperativity term (γ) that applies in the solid state [14, 15]

$$G = x_{HS}(\Delta H - T\Delta S) + \gamma x_{HS}(1 - x_{HS}) - TS_{mix} \quad (1)$$

where x_{HS} is the mole fraction of the HS phase; other symbols adopt their usual meaning.

Experimental

Preparations

Two samples were investigated experimentally in the present paper: $[Fe(bzimpy)_2](ClO_4)_2 \cdot 0.25H_2O$ (*bzimpy*=2,6-bis(benzimidazol-2-yl)pyridine) (**I**) and $[Fe(bzimpy_{-1H})_2] \cdot 2H_2O$ (*bzimpy*$_{-1H}$=deprotonated bzimpy) (**II**). The ligands and their complexes are shown in Fig. 1.

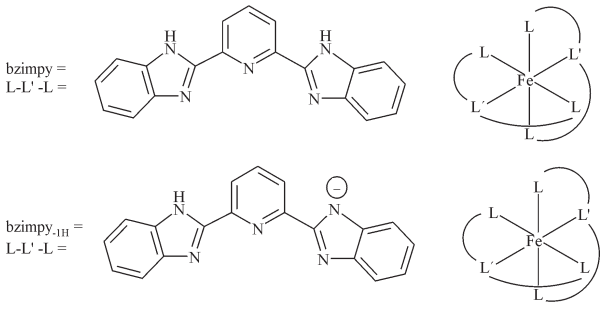

Fig. 1 Tridentate ligands and their complexes

The ligands and complexes were synthesized by previously described methods [4–6, 16, 17]. The crystal structures of **I** [16] and **II** [6] at room temperature have already been reported. C, H and N elemental analysis has been done for each sample and IR spectra at room temperature were scanned for analytical purpose.

Caution

On heating sample **I** can explode at temperature above 200°C owing to the presence of perchlorate. Heating until 200°C is safe.

Heat capacity measurements

The heat flow has been recorded using DSC calorimeter (Perkin Elmer, DSC-2 and DSC-7) with different scan rate s=5, 10 or 20°C min^{-1}. Three records have been scanned: (i) signal of the free aluminum pan; (ii) signal of the sample encapsulated in the pan; (iii) signal of the reference material – sapphire.

Powder diffraction study

X-ray powder patterns were scanned by the transmission diffractometer (STADIP, STOE) with CoK_α radiation (λ=1.78892 Å) in the range $6°<2\theta<45°$. The samples were heated until 443 K (**I**) and 523 K (**II**), respectively and then cooled to room temperature. Diagrams were collected in steps of 20 K.

Data processing

We will not differentiate among C_p, C_V, C_H and C_M for the solid-state samples through the paper.

The recorded heat flows were processed by the well known procedure to obtain the mass heat capacity of the sample [18]: (i) all isothermal edges were linearly transformed to the same origin; (ii) the sample holder signal subtracted from the sapphire and sample heat flows; (iii) the net sapphire heat flow and tabulated sapphire heat capacity used to calibrate the net sample heat flow into the heat capacity of the sample. The procedure assumes a constant waiting period before and after the heating and/or cooling and a constant temperature drift.

The Debye part due to molecular vibrations has been subtracted assuming that the functions $C_p=aT^3$ and $C_p/T=bT^2$ hold true. Thus a few data points below the onset temperature were used to determine the constants a_{LS} (b_{LS}) and a few data points above the transition to fit the constants a_{HS} (b_{HS}). Then the heat capacity was corrected for the underlying Debye part, which is different below and above the peak maximum T_{max}, hence

$$C'_p=C_p-a_{LS}T^3, \quad [\text{for } T<T_{max}] \tag{2a}$$

$$C''_p=C_p-a_{HS}T^3, \quad [\text{for } T>T_{max}] \tag{2b}$$

and

$$\left(\frac{C_p}{T}\right)' = \frac{C_p}{T} - b_{LS}T^2, \quad [\text{for } T<T_{max}] \tag{3a}$$

$$\left(\frac{C_p}{T}\right)'' = \frac{C_p}{T} - b_{HS}T^2, \quad [\text{for } T>T_{max}] \tag{3b}$$

Finally, the enthalpy and the entropy of the transition were evaluated numerically in two steps

$$\Delta H = \int_0^{T_{max}} C_p' \mathrm{d}T + \int_{T_{max}}^{\infty} C_p'' \mathrm{d}T \tag{4}$$

$$\Delta S = \int_0^{T_{max}} \left(\frac{C_p}{T}\right)' \mathrm{d}T + \int_{T_{max}}^{\infty} \left(\frac{C_p}{T}\right)'' \mathrm{d}T \tag{5}$$

The difference between the HS and the LS function is the excess enthalpy and the excess entropy, respectively. This is thought to be a step between extrapolated LS and HS curves just at T_c.

Results and discussion

According to magnetic susceptibility data (Fig. 2) the effective magnetic moment increases on heating to the value corresponding to four unpaired electrons (the spin-only value is μ_{eff}=4.9 μ_B). This evidences that the spin crossover (S=0 to S=2 spin transition) occurs. Some residual paramagnetism below the spin transition is due to the presence of a paramagnetic impurity – an Fe(III) admixture, which is difficult to eliminate completely during preparation, sample manipulation and it may be formed also owing to sample aging.

The first sample (sample **A** of **I**, fine powder material) was cycled on DSC-2. According to Fig. 3, there is an endothermic peak accompanied with a broad satellite in the heating direction. On cooling, only the first peak has its exothermic counterpart. We conclude, that the satellite at T_{p2}=424 K corresponds to some crystal water that was liberated at the end of heating. (The presence of some crystal water was confirmed by the single-crystal X-ray analysis. A more direct evidence for the powder sample is seen in the IR spectra: a broad band at 3300–3600 cm^{-1}, corresponding to the O–H stretching vibration, disappears at the first heating.) The principal endothermic peak corresponds to the first-order phase transition that accompanies the spin crossover. This well developed peak is recovered on a subsequent cycling (in both, heating and cooling directions). Notice that the temperature of the peak-maximum is different in the heating direction, $T_{p1}^{\uparrow}$=406 K, and the cooling direction, $T_{p1}^{\downarrow}$=398 K; such a difference remains on the second heating/cooling cycle. This feature matches the findings of the magnetic measurements, which show that a thermal hysteresis of the width of about ΔT=12 K exists in **I**.

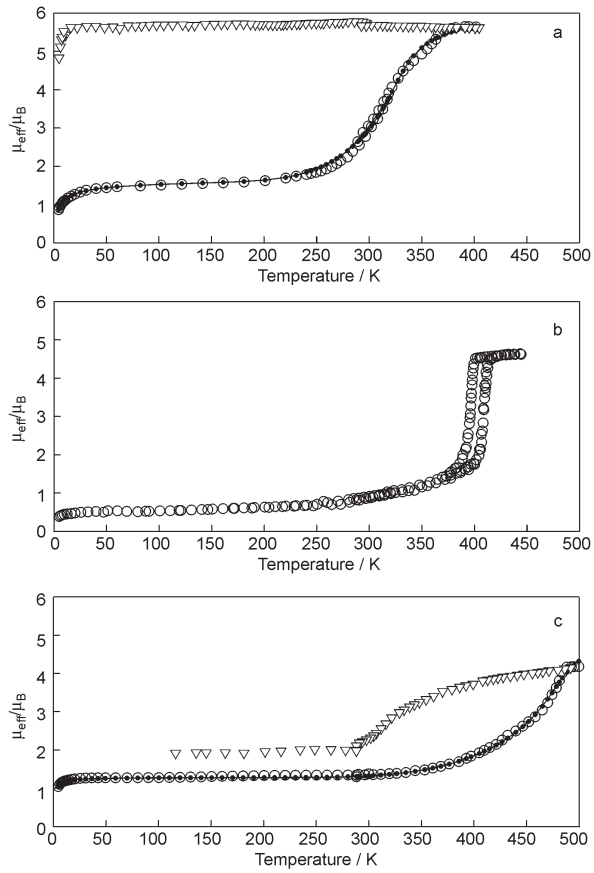

Fig. 2 Temperature dependence of the effective magnetic moment for Fe(II) complexes: a – $[Fe(bzimpy)_2](BPh_4)_2 \cdot 4H_2O$; b – $[Fe(bzimpy)_2](ClO_4)_2 \cdot 0.25H_2O$; c – $[Fe(bzimpy_{-1H})_2] \cdot H_2O$

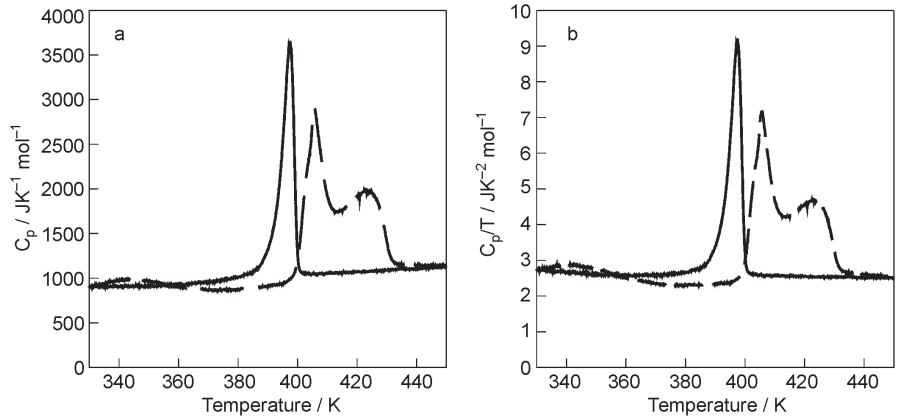

Fig. 3 Experimental heat capacity for sample **A** of **I** (a) and function (C_p/T) *vs.* T (b). Dashed – first heating; solid – first cooling. Conditions: DSC-2, s=5 K min^{-1}

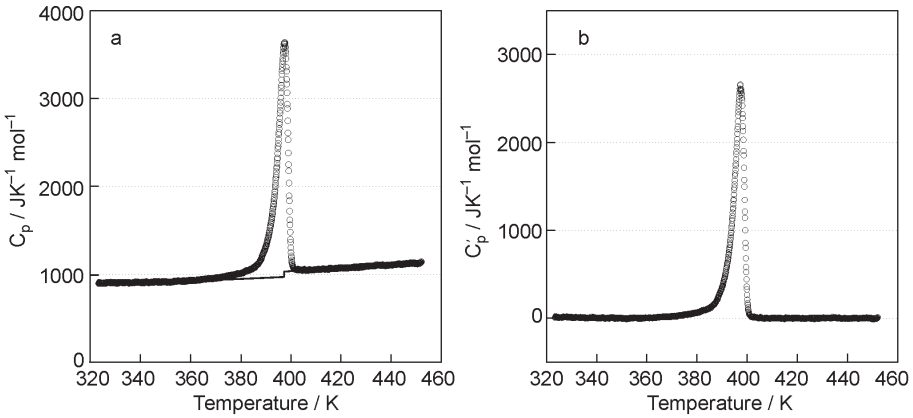

Fig. 4 Processing the heat capacity (sample **A** of **I**): a – fitting the LS and HS Debye part (lines); b – subtraction of the underlying Debye part prior to the integration yielding ΔH. Conditions: DSC-2, s=5 K min^{-1}

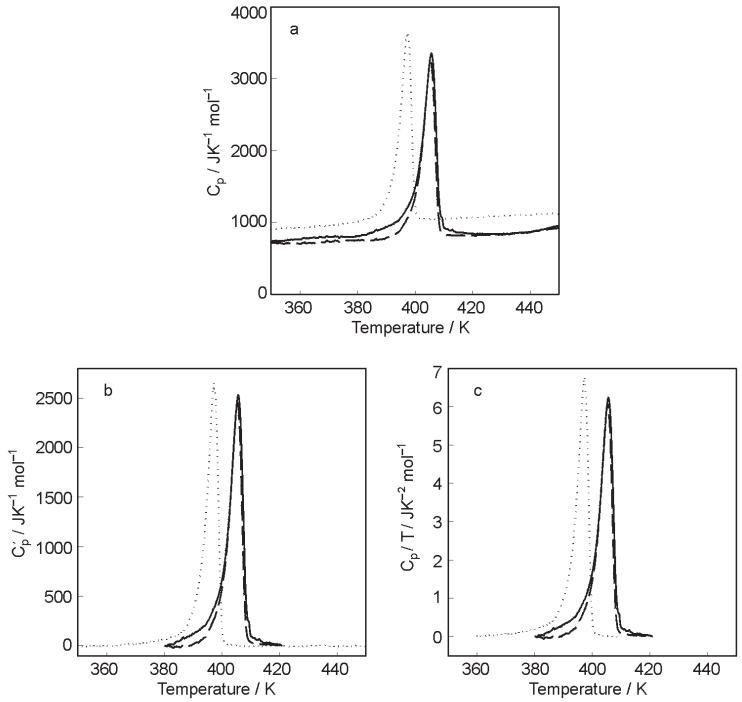

Fig. 5 a – measured temperature dependence of the heat capacity for **I**;
b – an under-integral enthalpic function ((C'_p/T) *vs.* T);
c – an under-integral entropic function (C_p *vs.* T)′. Dotted – powder sample **A** on the first cooling; solid – microcrystalline sample **B** on the first cooling; dashed – microcrystalline sample **B** on the second cooling. Conditions: s=5 K min^{-1}; **A** – DSC-2, **B**=DSC-7

The experimental data have been processed using Eqs (2)–(4). According to Fig. 4 the excess enthalpy (and analogously the excess entropy) represent only a minor correction in the present case. The numerical integration of the corrected C_p and C_p/T functions for the first cooling gave the enthalpy of the spin transition, ΔH=15.4 kJ mol^{-1}, and the entropy of the spin transition, ΔS = 40.0 J mol^{-1} K^{-1}.

From detailed magnetochemical investigations we know that samples of **I** may behave differently, depending on the method of preparation (microcrystalline material *vs.* fine powdered sample) and history of aging (presence of Fe(III) impurities). Therefore, the second sample (sample **B** of **I**, microcrystalline material) was cycled on DSC-7 and compared with the data obtained previously. According to Fig. 5 there is some shift of the peak-maximum temperature and the integration gave the results: ΔH=17.4 kJ mol^{-1} and ΔS=43.1 J mol^{-1} K^{-1} for the first cooling, and ΔH=14.0 kJ mol^{-1} and ΔS=34.6 J mol^{-1} K^{-1} for the second cooling. In both cases $\Delta H/\Delta S$=404 K that matches the peak maximum of T_{p1}=405 K.

The obtained values of ΔH=14–17 kJ mol^{-1} lie at the higher limit of experimental acquisition [19] whereas ΔS=35–43 J mol^{-1} K^{-1} span the centre of the published interval. The last value shows a considerable contribution of the molecular vibrations (the pure spin-multiplicity change yields $\Delta S_{spin}=R\ln 5$=13.4 J mol^{-1} K^{-1}).

Sample **II** was cycled three times between 300 and 580 K. In the first heating directions endothermic peaks were registered with the maxima at T_{p1}=425 K and T_{p2}=520 K (Fig. 6). No decomposition of the complex was registered at the highest limit of the thermal treatment by an independent TG study. Only a single endothermic peak at T_{p1}=425 K is recovered at the second and third heating. Taking into account the temperature dependence of the IR spectra, we can conclude that the second satellite corresponds to the liberation of the crystal water whereas the first peak is a first-order phase transition that accompanies the spin crossover.

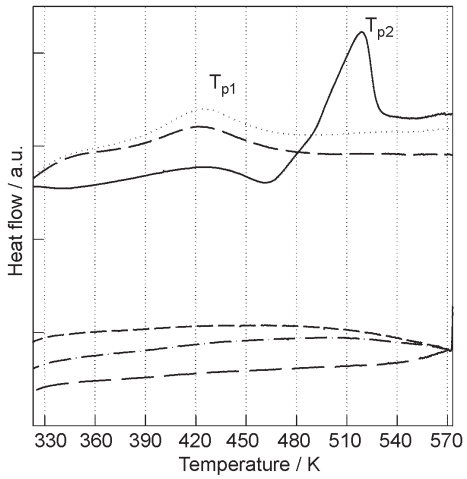

Fig. 6 Temperature dependence of the heat flow for sample **II** (scan rate s=10 K min^{-1}). Full line – the first heating, other lines – heating and/or cooling. The records were corrected for the baseline

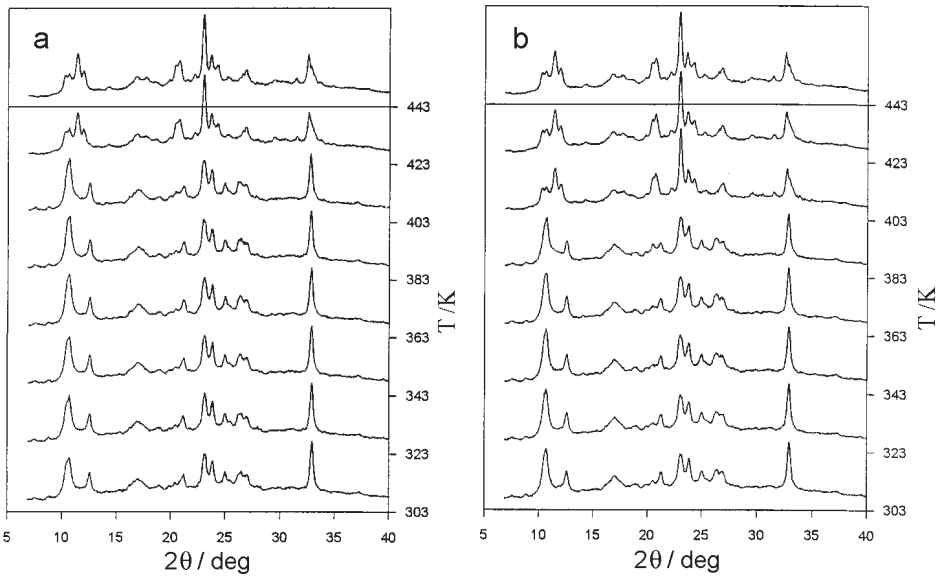

Fig. 7 Temperature dependence of the X-ray powder diffraction patterns for **I**. a – heating direction from bottom to top; b – cooling direction from top to bottom. (The reader is recommended to watch the figure at a very sharp angle for a better impression)

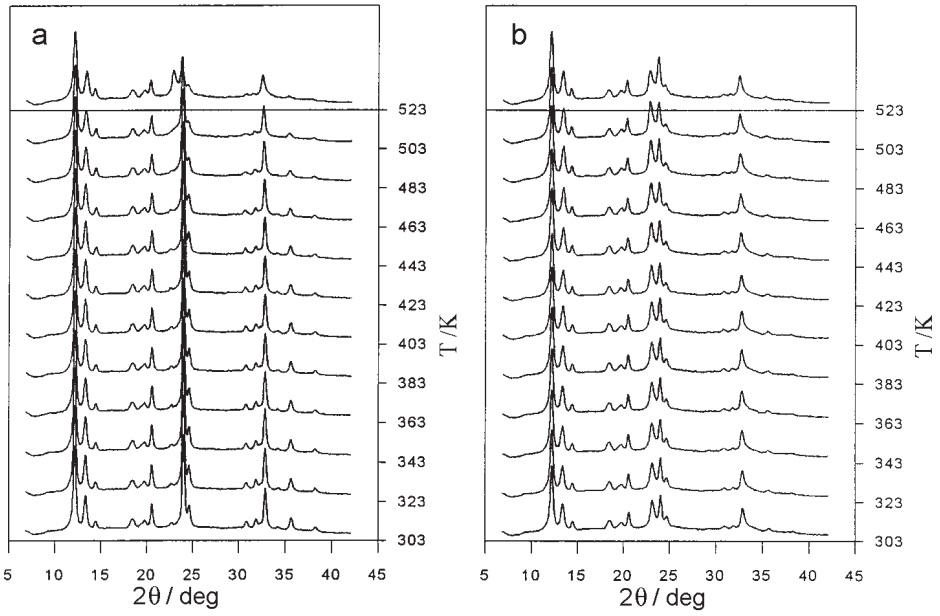

Fig. 8 Temperature dependence of the X-ray powder diffraction patterns for **II**. a – heating direction from bottom to top; b – cooling direction from top to bottom. (The reader is recommended to watch the figure at a very sharp angle for a better impression)

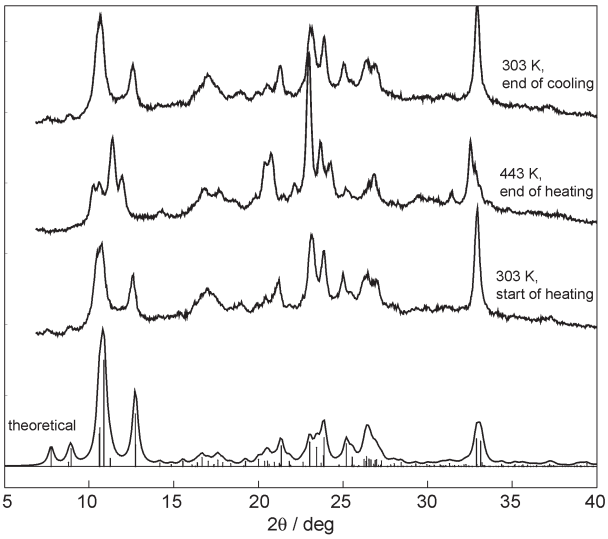

Fig. 9 Theoretical pattern for sample **I** based on the room-temperature X-ray structure [16] as compared to experimental data at different temperatures. Vertical lines – positions of the theoretical diffractions for a triclinic crystal system. Simple Lorenzian form of the peaks with a broadening of 0.2 deg was assumed

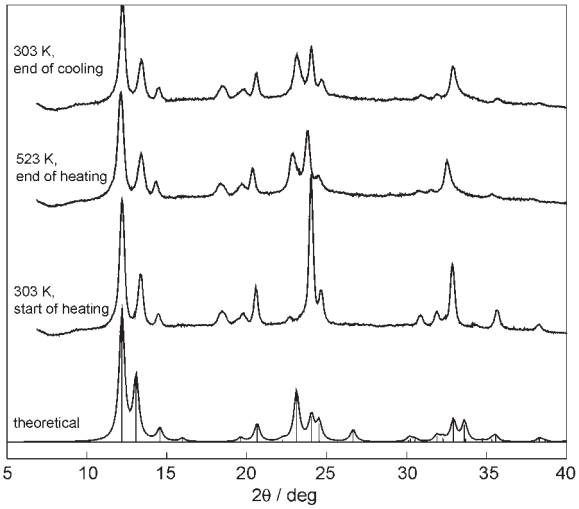

Fig. 10 Theoretical pattern for sample **II** based on the room-temperature X-ray structure [6] as compared to experimental data at different temperatures. Vertical lines – positions of the theoretical diffractions for a tetragonal crystal system. Simple Lorenzian form of the peaks with a broadening of 0.2 deg was assumed

The aspect, which is more difficult to understand, is the absence of the exothermic peak in the cooling direction when the sample is transformed back from the high-spin to the low-spin state. Perhaps the process is very gradual (owing to breaking the cooperativeness) so it is not resolved under the conditions of the DSC experiment.

The temperature evolution of the X-ray powder diffraction patterns is shown in Fig. 7 for **I** and Fig. 8 for **II**.

The changes in the relative intensities and the position of the X-ray patterns in the range $8°<2\theta<13°$ and $18°<2\theta<27°$ were found to be reversible for sample **I**. The liberation of a fractional content of water at the first heating is irrelevant to the spin crossover that stays well reproducible for **I**. The structural changes between 403 and 423 K fit well the spin transition identified by magnetic susceptibility measurements (Fig. 2) and DSC (Figs 3–5). Theoretical X-ray diffraction pattern (based on the room-temperature single crystal structure [16]) resembles the main features of the experimental diffractogram at room temperature (Fig. 9) and markedly differs from features at 443 K. The system probably remains triclinic.

The liberation of the crystal water from **II** at the first heating manifests itself in a change of the X-ray diffraction patterns. The change is irreversible – it remains constant on back cooling to the room temperature (Fig. 10). Although the structural changes are evident, the system probably remains tetragonal. (The feature at $2\theta=19°$ is clearly an artifact of the applied hardware.)

Conclusions

$[Fe(bzimpy)_2](ClO_4)_2 \cdot 0.25H_2O$ and $[Fe(bzimpy_{-1H})_2] \cdot H_2O$ exhibit thermally induced spin transition evidenced by the magnetic susceptibility measurements. DSC data show that an endothermic peak corresponding to the first-order phase transition accompanies the spin crossover. While the entropy of the spin transition of about ΔS~40 J mol^{-1} K^{-1} spans quite typical value, the enthalpy ΔH~15 kJ mol^{-1}, on the contrary, lies at the higher limit of available experimental data. Such an enthalpic disfavor of the spin crossover is the raison d'être of the very useful property: the shift of the transition temperature above the room temperature.

References

1 O. Kahn, J. Kröber and C. Jay, Adv. Mater., 4 (1992) 718.
2 D. Gatteschi, Adv. Mater., 6 (1994) 635.
3 O. Kahn and C. J. Martinez, Science, 279 (1998) 44.
4 R. Boča, P. Baran, M. Boča, L. Dlháň, H. Fuess, W. Haase, W. Linert, B. Papánková and R. Werner, Inorg. Chim. Acta, 278 (1998) 190.
5 R. Boča, M. Boča, L. Dlháň, K. Falk, H. Fuess, W. Haase, R. Jaroščiak, B. Papánková, F. Renz, M. Vrbová and R. Werner, Inorg. Chem., 40 (2001) 3025.
6 R. Boča, F. Renz, M. Boča, H. Fuess, W. Haase, G. Kickelbick, W. Linert, G. Miehe, B. Papánková, M. Vrbová and R. Werner, Inorg. Chem., submitted.

7 R. L. Carlin and A. J. van Duyneveldt, 'Magnetic Properties of Transition Metal Compounds', Springer, New York 1977.
8 R. L. Carlin, 'Magnetochemistry', Springer, Berlin 1986.
9 D. C. Mattis, 'The Theory of Magnetism II', Springer Series in Solid-State Sciences 55, Springer, Berlin 1985.
10 D. Craik, 'Magnetism', Wiley, Chichester 1995.
11 R. Boča, Coord. Chem. Rev., 173 (1998) 167.
12 R. Boča, 'Theoretical Foundations of Molecular Magnetism', Elsevier, 1999.
13 M. Sorai and S. Seki, J. Phys. Chem. Solids, 35 (1974) 555.
14 O. Kahn, 'Molecular Magnetism', VCH, New York 1993.
15 C. Cantin, J. Kliava, A. Marbeuf and D. Mikailitchenko, Eur. Phys. J., B12 (1999) 525.
16 R. Boča, P. Baran, L'. Dlháň, H. Fuess, F. Renz, W. Linert, I. Svoboda and R. Werner, Inorg. Chim. Acta, 260 (1997) 129.
17 M. Vrbová, Ph.D. Thesis, STU Bratislava 2000.
18 G. Höhne, W. Hemminger and H. J. Flammersheim, 'Differential Scanning Calorimetry', Springer, Berlin 1996.
19 E. König, Struct. Bonding, 76 (1991) 51.